論文 A Research on the Seismic Behavior of Precast Concrete Columns Using High-Strength Shear Reinforcement

Primo Allan ALCANTARA*1, Juan Jose CASTRO*2, Teruaki YAMAGUCHI*2 and Hiroshi IMAI*3

ABSTRACT: This research aims on further investigating the structural performance of the so-called *main bar post-insertion method* as applied to precast concrete columns. This type of joint method features the use of spiral steel sheaths which are hollow tubes positioned in place of the main bars that are to be later inserted during assembly. Also, its main objective is to determine the influence of the strength and amount of lateral reinforcement to the seismic behavior of precast concrete columns.
KEYWORDS: precast concrete column, shear reinforcement, ultimate strength capacity, spiral steel sheath, yield strength

1. INTRODUCTION

In Japan, the precast concrete construction of frame type structures developed from the column tree type (early 1970's) to the single member type (late 1970's) to the exterior shell type (1980's). However, in the 1990's, considering the advantages and disadvantages of the above-mentioned construction types brought about the introduction of the *main bar post-insertion method* [1] as shown in Fig. 1. The main bar post-insertion method is described as the process wherein, at the factory, the structural members are prefabricated without the presence of the main bars, and later at the construction site, the main bars are inserted and abutted at the middle portion of each member where the stresses due to seismic forces are small. This type of joint features the use of spiral steel sheaths which are hollow tubes positioned in place of the main bars in precast concrete members wherein such bars are to be later inserted during assembly.

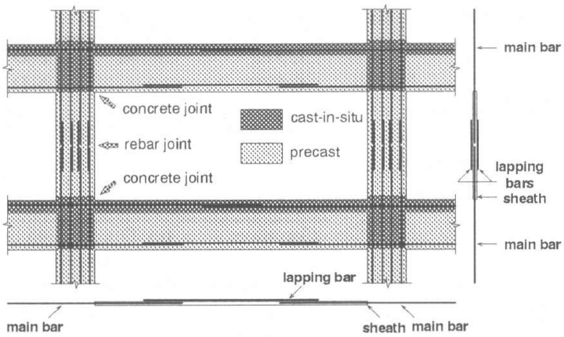

Fig. 1 Main Bar Post-Insertion Method

2. EXPERIMENTAL BACKGROUND

The pioneering experiment done on the seismic performance of precast concrete columns using the main bar post-insertion method was done in 1990 [2]. The series dealt with a different type of casting method called centrifugation. In 1991, the second series was tested [3]. Specimens were cast in an ordinary manner and focused mainly on the influence of two parameters, shear reinforcement ratio, Pw, (0.3~0.8%) and axial loading. Their major objective was to investigate the

*1 Graduate School, University of Tsukuba, Member of JCI
*2 Technical Research Institute, Kabuki Construction Co. Ltd., Member of JCI
*3 Institute of Engineering Mechanics, University of Tsukuba, Member of JCI

structural performance of precast concrete columns with lapping joints at midheight subjected to shear forces. Since the scope of the second series dealt only with columns having low shear reinforcement ratios, it was necessary to consider those having a larger amount of shear reinforcement. Thus, in 1994, a third series was performed [4]. It focused on the investigation of the structural performance of precast concrete columns having higher shear reinforcement ratios (0.6~1.5%). The latest experiment, done in 1996, aims on further investigating the application of the main bar post-insertion method to precast concrete columns. Here, the main parameters are the strength and amount of lateral or shear reinforcement.

3. SPECIMEN DETAILS

A total of 10 specimens were fabricated consisting of 6 precast concrete and 4 monolithic types. In order to simulate earthquake movements on a column, these specimens were subjected to cyclic shear forces as well as a relatively high axial load. Figure 2 shows a layout of the column specimens while the specification details are found on Table 1. For this series, continuous main bars were adapted for a better evaluation of the performance of the spiral steel sheaths.

The columns differ in the amount and strength of lateral or shear reinforcement used. This is done by varying the number of lateral ties as well as the hoop spacing. Also, to investigate the effect of using high strength shear reinforcement, two types of high strength bars were used.

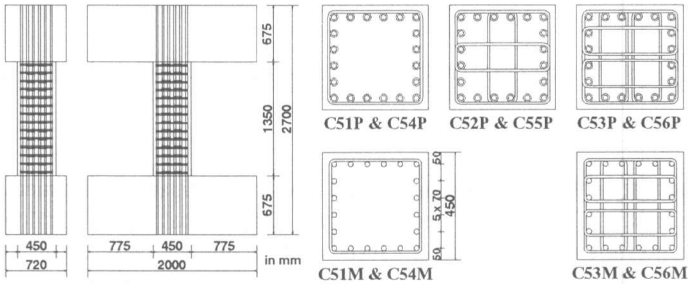

outline cross section

Fig. 2 Column Specimen

Table 1 Column Specifications

Specimen Precast	Specimen Monolithic	Shear Reinforcement	Pw %	yield strength σ_{wy}	Axial Load kgf/cm^2
C51P	C51M	2-D10@100	0.32		60
C52P	-	4-D10@100	0.63	SD785	"
C53P	C53M	6-D10@80	1.19		"
C54P	C54M	2-D10@100	0.28		"
C55P	-	4-D10@100	0.57	USD1275	"
C56P	C56M	6-D10@80	1.07		"
Common:	b x D x h :	45 cm x 45 cm x 135 cm		sheath :	
	main bars :	20-D22 (SD 685)		diameter	34 mm
	lateral reinforcement :	D10 (σ_{wy})		lug height	2 mm
	design concrete strength :	300 kgf/cm^2		pitch	28 mm
	design grout strength :	600 kgf/cm^2			

4. MATERIAL PROPERTIES

Table 2 shows the test results of the reinforcing bars, concrete and grout used. In actual design practice, ordinary strength bars are used for main bars, but for experimental purposes, high strength bars were used.

5. TEST METHOD

Each of the column specimens was set under the loading apparatus shown in Fig. 3. These specimens were subjected to varying shear forces that were applied in a cyclic manner producing anti-symmetric bending moment distribution while being acted upon by a constant axial load. Each specimen was set using oil jacks found on both sides of the upper and lower beams. Here, the shear force was applied through the horizontal actuator while the axial load was provided by the two vertical actuators shown. For the proper simulation of seismic behavior, each specimen was made to drift once at a drift angle R equal to ±1/800, then twice at R of ±1/400, ±1/200, ±1/100 and ±1/50 and again once at R equal to ±1/25. To follow the prescribed loading history, displacement transducers were installed on both sides of the specimen. Along the height of the column, clip gauges were systematically arranged to measure local deformation. Asides from these, strain gauges were strategically positioned all over the reinforcing bars of the specimen.

Table 2 Material Test Results

(a) Reinforcing Bars (tonf/cm^2)

Size	Grade	Young's Modulus	Yield Stress	Tensile Stress	Elongation %	Remarks
D22	SD685	1.89x10^3	7.36	9.95	8.3	Main
D10	SD785	2.20x10^3	9.14	11.04	13.0	Hoop
D10	USD1275	2.05x10^3	13.81	14.83	5.2	Hoop

(b) Concrete (kgf/cm^2)

Specimen	Compression	Split
C51P & C52P	376	28.5
C53P & C54P	426	29.8
C55P & C56P	412	30.6
C51M & C53M	377	23.2
C54M & C56M	371	24.3

(c) Grout (kgf/cm^2)

specified strength	600
7 days	611
28 days	717
55 days	740
63 days (last day of expt)	741

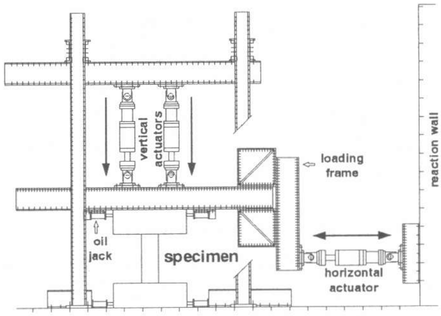

Fig. 3 Loading System

6. EXPERIMENTAL RESULTS AND ANALYSIS

6.1 PROGRESS OF THE EXPERIMENT

For all specimens, initial cracking due to flexure occurred during the 1/800 cycle. At R=1/400, extensions of the initial cracks or shear-flexural cracks appeared. Also, at this stage, initial shear cracking commenced but only for specimens having the least amount of shear reinforcement or low Pw (≦0.32, namely C51 & C54 types) as well as for all the monolithic specimens and for the rest it occurred at R=1/200. It was also at this cycle that bond failure occurred for the low Pw monolithic specimens due to the fact that the peak load was already attained as well as the appearance of bond splitting cracks along the extreme row of main bars. And for the low Pw precast types, this condition occurred at the 1/100 cycle. The progress of the bond splitting cracks became more and more prominent for the succeeding cycles coupled with the spalling of the concrete. For the specimens C52P and C55P, shear and bond splitting cracks progressed at the 1/100 cycle and peak load was attained at R=1/50 with the bond splitting cracks becoming more prominent as well as the spalling of concrete. This continued until R=1/25.

Lastly, for the high Pw specimens, shear cracking continued for R=1/100 and 1/50 cycles. It was also at the R=1/50 stage that there were yielding of the extreme row of main bars and crushing of concrete at the top and bottom portions of the column leading to flexural failure. In addition, peak load was already attained for the monolithic types whereas this occurred at R=1/25 for their precast counterparts. Moreover, at this stage, bond splitting cracks could be seen at the sides of the specimens as well as further crushing of the concrete. A comparison of the bond splitting (C51P & C54P) and flexural failure types (C53P & C56P) is shown in Fig. 4.

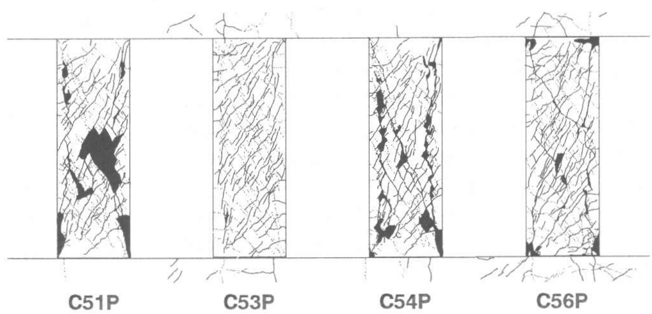

Fig. 4 Crack Patterns

6.2 LOAD-DISPLACEMENT CURVES

Figure 5 shows relationships between the applied shear force and the horizontal displacement or drift angle. The curve depicted by specimen C51P represents the bond splitting failure type while that of C53P shows the flexural failure type. It was observed that the curve of the bond splitting type peaked at the an earlier stage than that of the flexural type. A comparison of these curves with those of the specimens having shear reinforcement of higher yield strength as well as their monolithic counterparts could be shown from the envelope curves found in Fig. 6. Considering the shape as well as the magnitude of the shear load, there is not much difference for the specimens using SD785 ($\sigma_{wy} \fallingdotseq 25\sigma_B$) compared to the ones using USD1275 ($\sigma_{wy} > 25\sigma_B$). Also, according to the casting method, there is not much difference between the precast concrete and monolithic types.

6.3 PARTIAL DEFORMATION

In order to calculate the deformation components due to shear and flexure, it is necessary to first determine the shear distortion and curvature values at specific locations along the height of the column. Representative graphs showing these values are shown in Fig. 7. With regard to the distortion values, they tend to become large at the middle portion of the specimen which is mainly due to the presence of shear cracks. On the other hand, the curvature distribution is very much similar to the assumed bending moment diagram. Calculations using such shear distortions and curvatures give partial deformations due to shear and flexure, respectively. A typical diagram showing shear and flexure deformation components is also shown in Fig. 7. Here it could be seen that there is no significant difference between precast and monolithic specimens with these aspects. Lastly, these deformations would add up to the calculated total deformation on the column which is very close to the actual relative displacement between the upper and lower beams as shown also in Fig. 7.

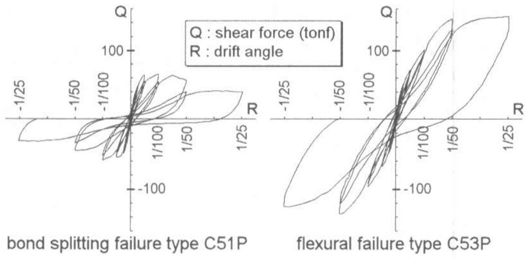

Fig. 5 Shear Force-Drift Angle Curves

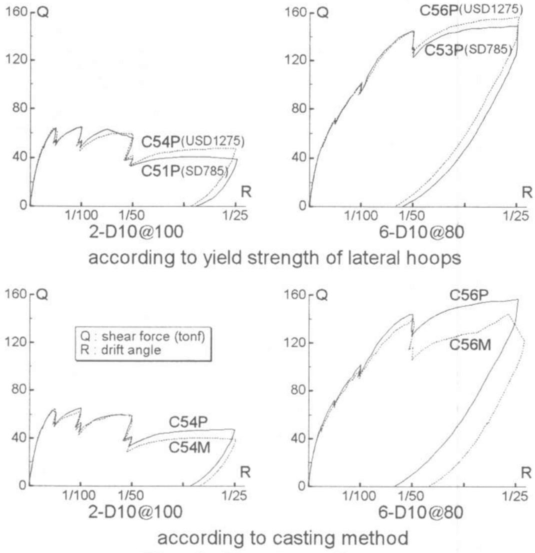

Fig. 6 Envelope Curves

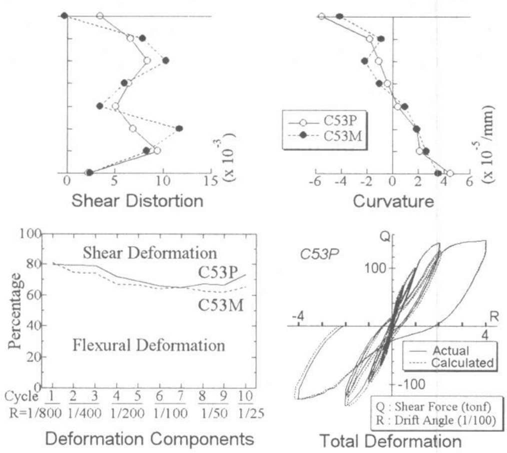

Fig. 7 Partial Deformation

6.4 STRAIN DISTRIBUTION

Representative graphs showing the strain distribution on the main bars are shown in Fig. 8. Focusing on the left-hand graph, it could be observed that the strain distribution on a corner main bar for the bond splitting failure type is straight and has not yielded which suggests the validity of the assumed bending moment distribution. On the other hand, for the flexural failure type, there is yielding at the end portions of the column. Continuing to the right-hand graph, it was observed from the strain distribution of the main bars at the end portion of the column that the plane sections remain plane assumption is valid for both SD785 and USD1275 types of specimens. Also, the main bar strain distribution of precast concrete specimens is very much similar to that of their monolithic counterparts which suggests adequate performance of the spiral steel sheaths under seismic loading.

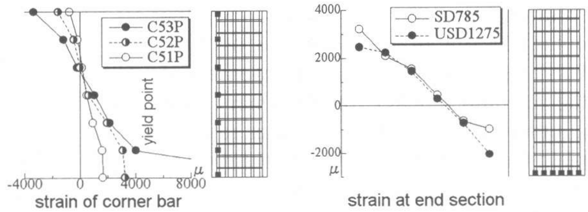

Fig. 8 Main Bar Strain Distribution

With regard to the strain distribution on the lateral hoops, it could be observed from Fig. 9 that there is no yielding at peak loading for both strength types as well as for both the bond splitting and flexural failure types. Thus, it can be stated that shear failure has not occurred. Also, there is not much difference between the precast and monolithic specimens based on the strain distribution on the hoops.

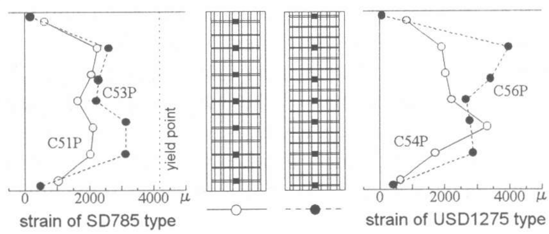

Fig. 9 Lateral Hoop Strain Distribution

7. ULTIMATE STRENGTH

Table 3 shows the ultimate strength calculations and experimental results for the specimens. The shear capacity was calculated using the strength equation (method A) given in the Architectural Institute of Japan's Ultimate Strength Design Guidelines [5]. On the other hand, the bond splitting capacity was obtained using the equation proposed by Kaku [6] wherein the bond strength is calculated using the sheath diameter as the main bar diameter for the precast concrete specimens since the combination of the sheath, grout and main bar acts as a unit. Also, the calculation of the flexural capacity is based on the ultimate strength concept using the strain compatibility assumptions. The resulting failure mode is actually based on the observed crack patterns and strain distributions on the steel reinforcements. From the table, it could be observed that all the specimens should have failed in bond splitting. However, only the specimens having the least amount of reinforcement have the good agreement with the experimental values while the rest showed higher bond splitting strength than their calculated values. It is worth

Table 3 Ultimate Strength

(tonf)

Specimen	p_w (%)	Calculated Values: Shear Capacity	Bond Splitting Capacity	Flexural Capacity	Test Results	Failure Mode
C51P	0.32	99.3	59.7	145.9	65.2	Bond
C52P	0.63	139.1	73.8	145.9	106.4	Bond
C53P	1.19	163.4	108.5	149.0	149.3	Flexure
C54P	0.28	104.6	63.4	149.0	65.4	Bond
C55P	0.57	145.2	75.8	148.2	102.5	Bond
C56P	1.07	160.3	101.7	148.2	156.8	Flexure
C51M	0.32	99.3	60.6	145.9	65.9	Bond
C53M	1.19	151.9	103.5	145.9	145.1	Flexure
C54M	0.28	92.9	59.1	145.6	64.8	Bond
C56M	1.07	150.4	97.9	145.6	145.2	Flexure

noting that in the calculation of the bond splitting capacities of columns, only the outermost row of main bars was used (6-bars). But considering the arrangement of the column's main reinforcement, the number and location of the inner rows of main bars could be said to be contributory to the bond splitting strength. Lastly, Fig. 10 shows the behavior of the ultimate strength in terms of the shear loading against the lateral reinforcement ratio, p_w, Included in the graph is the theoretical bond splitting strength considering the presence of the succeeding two inner rows of main bars (10-bars). Here, it could be observed that the specimens with a large amount of lateral reinforcement gave bond splitting capacities greater than their flexural strengths and hence, flexural failure. However, the bond splitting strengths for the specimens having the least amount of lateral reinforcement shows a little overestimation with the main difference in the design lying on the number of inner lateral hoops used. Thus, it could be inferred that presence of inner hoops as well as that of the inner main bars greatly influences the bond splitting capacities in columns. Another observation is that the capacity of the specimens having lateral hoops of higher strength is very much identical to that of those using a lower strength. Lastly, these is little discrepancy between the actual capacities of the precast concrete and the monolithic specimens.

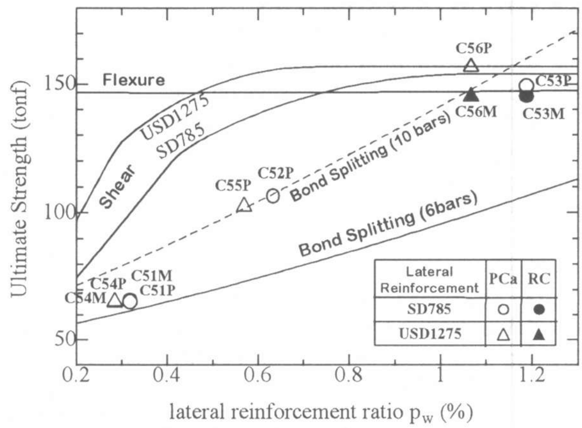

Fig. 10 Ultimate Strength

8. CONCLUSIONS

The following could be concluded from the analysis of the experiment made:

a) The seismic performance of precast concrete columns using the main bar post-insertion method is similar to that of monolithic columns based on the strength and amount of lateral reinforcement.

b) Considering the ultimate strength as well as the overall performance of the columns, there is not much difference between the specimens using SD785 compared to the ones using USD1275.

c) The presence of the inner rows of main bars as well as the inner lateral hoops could greatly influence the bond splitting capacities of columns.

REFERENCES

(1) Imai, H., "Precast Method for Frame Type Buildings", Structural Failure, Durability and Retrofitting, Vol. 4, 1993, pp. 396-403.

(2) Kobayashi, T., Yamaguchi, T., and Imai, H., "Shear Performance of Centrifuged Precast Columns with Lapping Joints", Transactions of the Japan Concrete Institute, Vol. 13, 1991, pp. 589-596.

(3) Kobayashi, T., et al., "An Experimental Study on the Seismic Performance of Precast Concrete Columns under Shear Forces", Transactions of the Japan Concrete Institute, Vol. 14, 1992, pp 409-416.

(4) Alcantara, P.A., et al., "A Study on the Influence of Shear Reinforcement Ratios of the Seismic Performance of Precast Concrete Columns", Transactions of the Japan Concrete Institute, Vol. 17, 1995, pp. 173-180.

(5) Architectural Institute of Japan, "AIJ Structural Design Guidelines for Reinforced Concrete Buildings", 1994, pp. 77-123.

(6) Kaku, T., et al, "The Proposal of Equation for Bond Splitting Strength of Reinforced Concrete Members Including High Strength Concrete Level", Concrete Research and Technology, Vol. 3, No. 1, 1992, pp. 97-108.